ACS OMEGA

http://pubs.acs.org/journal/acsodf

Article

Synthesis and Characterization of Functionalized Amino Dihydropyrimidines Toward the Analysis of their Antibacterial Structure−Activity Relationships and Mechanism of Action

Zachary W. Boyer,[#] Hannah Kessler,[#] Hannah Brosman, Kirsten J. Ruud, Alan F. Falkowski, Constance Viollet, Christina R. Bourne, and Matthew C. O'Reilly*

Cite This: *ACS Omega* 2022, 7, 37907−37916

Read Online

ACCESS | Metrics & More | Article Recommendations | Supporting Information

ABSTRACT: Antibiotic resistance among bacteria puts immense strain on public health. The discovery of new antibiotics that work through unique mechanisms is one important pillar toward combating this threat of resistance. A functionalized amino dihydropyrimidine was reported to exhibit antibacterial activity via the inhibition of dihydrofolate reductase, an underexploited antibacterial target. Despite this promise, little is known about its structure−activity relationships (SAR) and mechanism of activity. Toward this goal, the aza-Biginelli reaction was optimized to allow for the preparation of focused libraries of functionalized amino dihydropyridines, which in some cases required the use of variable temperature NMR analysis for the conclusive assignment of compound identity and purity. Antibacterial activity was examined using microdilution assays, and compound interactions with dihydrofolate reductase were assessed using antimicrobial synergy studies alongside *in vitro* enzyme kinetics, differential scanning fluorimetry, and protein crystallography. Clear antibacterial SAR trends were unveiled (MIC values from >64 to 4 μg/mL), indicating that this compound class has promise for future development as an antibacterial agent. Despite this, the *in vitro* biochemical and biophysical studies performed alongside the synergy assays call the antibacterial mechanism into question, indicating that further studies will be required to fully evaluate the antibacterial potential of this compound class.

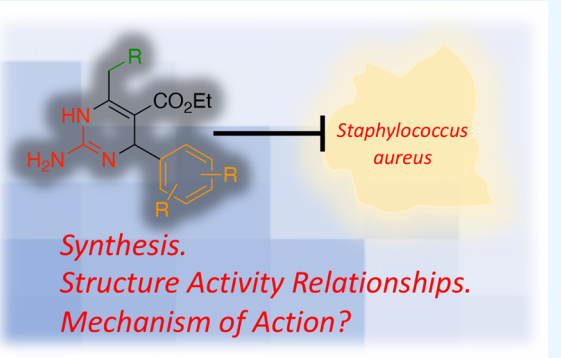

INTRODUCTION

Recent numbers from the United States Centers for Disease Control (CDC) estimate that over 2.8 million people acquire antibiotic-resistant (AR) bacterial infections each year.[1−3] While the 2019 CDC report[3] declined to assign a financial cost of antibiotic resistance, previous studies have estimated the cost of AR bacteria in the United States to be much as 35 billion dollars per year because of factors including extended hospital stays, costlier interventions, and increased number of follow-up visits.[2] Among the AR bacterial threats that the CDC has deemed "serious", methicillin-resistant *Staphylococcus aureus* (MRSA) is particularly concerning, as it causes slightly less than one-third of the overall deaths associated with AR organisms.[3] AR pathogens place an immense strain on public health, and it is critical that antibiotics targeting new or underexploited targets are developed to mitigate this threat.

Dihydrofolate reductase (DHFR) is an enzyme that catalyzes the reduction of dihydrofolate to tetrahydrofolate, which is an important cofactor involved in essential cellular processes including the biosynthesis of DNA and amino acids.[4] The inhibition of DHFR halts cellular growth, which is the basis for DHFR's role as a drug target across multiple disease states, including antibacterial therapies. While many U.S. Food and Drug Administration (FDA)-approved medications exist among other antibiotic classes (e.g., around 40 β-lactam antibiotics),[5,6] trimethoprim (TMP, **1**) is the only approved antibacterial therapeutic that inhibits DHFR, demonstrating that it is a comparatively underexploited antibiotic target. Beyond TMP, mammalian DHFR is targeted by pharmaceutical methotrexate (MTX, **2**), and protozoal DHFR is targeted by pyrimethamine **3**. All these DHFR-inhibiting compounds have a common aminopyrimidine moiety that bears some structural resemblance to the reported functionalized dihydropyrimidine **4**, a compound with antibacterial activity against various strains of MRSA (Figure 1).[7] It is known that the aminopyrimidine ring in **1**−**3** is largely responsible for the competitive mode of DHFR inhibition, as it plunges into the active site in place of the pyrimidine ring present in DHFR's

Received: August 8, 2022
Accepted: October 4, 2022
Published: October 13, 2022

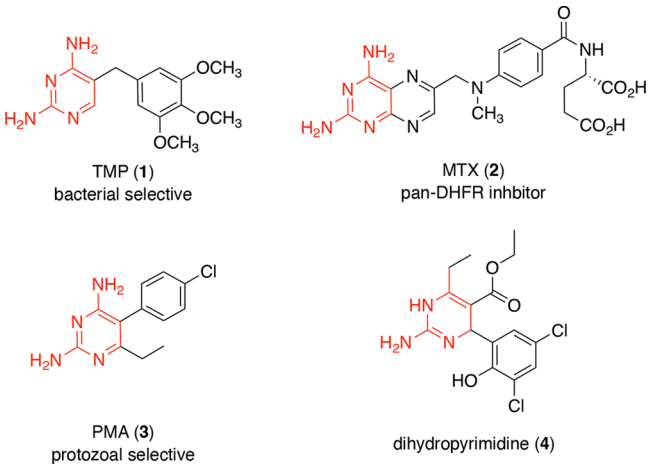

Figure 1. Structural similarities between FDA-approved pharmaceuticals targeting different DHFR isoforms (**1**–**3**) and the functionalized dihydropyrimidine **4**, the emphasis of this study.

substrate dihydrofolate.[8,9] Despite this common structural component, the selective competitive inhibition of bacterial DHFR can occur; TMP binds tightly to bacterial DHFR and very poorly to mammalian DHFR,[10−12] allowing TMP to generate selective bacterial toxicity. Comparatively, methotrexate is known as a pan-DHFR inhibitor, as it is highly potent at all isoforms. Other modes of DHFR inhibition may provide similar selectivity to TMP, as mechanisms could exist that target portions of DHFR that are less conserved than the active site. Along those lines, compound **4** was reported as an uncompetitive inhibitor of *S. aureus* DHFR,[7] making it a useful starting point toward the development of antibacterial agents that inhibit the underexploited antibiotic target DHFR.

Dihydropyrimidine **4** represents a solid lead compound for antibacterial development, as it was reported to display significant inhibition of various *S. aureus* strains (MIC values from 2 to 9 μg/mL (5.5−25 μM)), a lack of mammalian toxicity, no inhibition of bovine DHFR, and inactivity in a range of cross-indication assays used to investigate common cytotoxicity modes (up to 100 μM concentrations).[7] Despite that promise, limited direct analogues of **4** have been synthesized to investigate its structure activity−relationships (SAR) or mechanism of action, and no follow-up studies have been published since the original report. Herein, the synthesis of focused libraries modifying the different structural components of **4** are disclosed. Further, the antibacterial properties of the dihydropyrimidine scaffold are validated and compounds with enhanced or diminished antibacterial potency uncovered, elucidating the SAR. *In vitro* biochemical and biophysical studies performed alongside checkerboard assays to examine the synergy in the folate pathway then called the antibacterial mechanism into question, indicating that further studies will be required to fully evaluate the antibacterial potential of this compound class.

RESULTS AND DISCUSSION

Chemical Synthesis and Optimization. Dihydropyrimidine **4** is densely functionalized, containing guanidine, phenol, ester, and halogens on the arene ring. A significant amount of work has described the preparation of these dihydropyrimidine-containing compounds, the synthesis of which often hinges on the aza-Biginelli reaction, a three-component reaction involving guanidine, a β-keto ester, and an aldehyde. The seminal work on dihydropyrimidine **4** involved a modified aza-Biginelli reaction,[7,13] where the three components were combined under basic conditions ($NaHCO_3$) in dimethylformamide and heated to 70 °C (Scheme 1a). This enabled the

Scheme 1. Literature Precedent for Dihydropyrimidine Synthesis

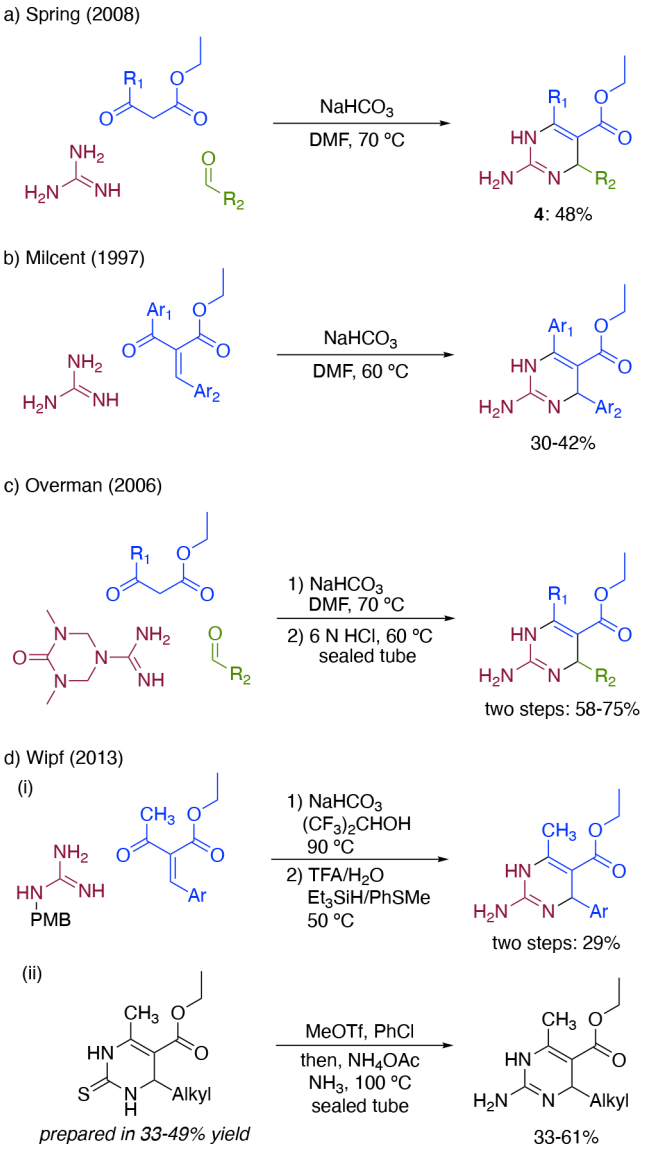

production of an array of dihydropyrimidines, where R_1 and R_2 included either arenes or alkyl chains (although limited SAR information was disclosed). The generality, efficiency (yields generally >50%) and simplicity of the synthesis is noteworthy, as the authors indicate that the products were purified by a simple precipitation upon addition to water, followed by collection of the analytically pure solid that was produced. Indeed, many previous methods required more complex purification procedures, including additional filtration, trituration, recrystallization, or chromatography steps, and most often provided yields in the range of <20%.[14−17] Milcent[18] reported the production of analytically pure aza-Biginelli products (30−42% yield) after various filtration steps under very similar reaction conditions to Spring,[7] although they

https://doi.org/10.1021/acsomega.2c05071
ACS Omega 2022, 7, 37907−37916

reacted the Knoevenagel adduct of the benzaldehyde and the β-keto ester with guanidine (Scheme 1b). Further, their substrates were limited to arene rings in the R_1 and R_2 positions, while the described procedure to access **4** required a tolerance for alkyl β-keto esters. Overman and co-workers further noted challenges associated with accessing dihydropyrimidine aza-Biginelli products that were alkyl-substituted. To address this challenge, they developed a procedure that employed a triazone-protected guanidine to facilitate access to substituted dihydropyrimidines with aryl or the more elusive alkyl substituents (two-step yields of 58−75% for alkyl substituents, Scheme 1c).[19] Unfortunately, the preparation of the triazone guanidine precursor required four-steps (38% overall) and a hydrogenolysis reaction with hydrogen under 750 psi, which limited our preparation of this useful intermediate. Wipf and co-workers similarly noted the challenge of accessing alkyl-substituted dihydropyrimidines; to address this, they developed one method of introducing a singular alkyl group in the R_1 position (Scheme 1d(i)) and a second method to allow the preparation of bisalkyl-substituted amino dihydropyrimidines (Scheme 1d(ii)).[20] Two recent reports that use sonication[21] or microwave irradiation[22] align more closely with the simplicity noted in the initial report of **4**[7] where the authors reported highly general methods capable of accessing both alkyl- and aryl-substituted dihydropyrimidines in high yields despite changing only the solvent and energy input methods (and lacking a thorough description of purification).[21,22] In sum, despite significant work describing access to functionalized amino dihydropyrimidines, questions remained regarding which conditions would most efficiently allow access to dihydropyrimidine **4** and analogues thereof.

Toward the synthesis of amino dihydropyrimidines, we initially investigated conditions identical to those in the report on the synthesis of **4**[7] by mixing guanidine **5**, 3,5-dichlorosalicylaldehyde **6**, and ethyl propionylacetate **7** with $NaHCO_3$ in anhydrous DMF at 70 °C for 16 h (Scheme 2a, detailed description of compound synthesis is provided in the Supporting Information). We were pleased to isolate a yellow solid that represented a 61% yield after aqueous precipitation and filtration under these conditions, close to the 48% yield noted in the literature.[7] Unfortunately, ^{1}H NMR examination indicated the product was likely present as a component of a quite complex mixture (Figure S1). To simplify things, we utilized the same conditions but included ethyl benzoylacetate **8** in place of **7** and 3,5-dichlorobenzaldehyde **9** in place of **6** (Scheme 2b). We expected these modifications to provide a more efficient reaction, as literature reports[18−20] indicated that aryl-substituted β-keto esters generally led to more efficient aza-Biginelli reactions. Further, we found no additional literature reports indicating that aza-Biginelli reactions worked efficiently with phenol-containing benzaldehydes. While this reaction also led to a complex mixture after a water precipitation and filtration, a precedented[18] secondary trituration of the primary filter cake utilizing organic solvents (dichloromethane) solubilized the impurities, allowing for the isolation of insoluble pure dihydropyrimidine **10** in a 55% yield. Encouraged by this outcome, this trituration purification method was applied to the synthesis of compound **4**, but no consistent, reliable purification was accomplished. To distinguish whether the differences in reaction efficiency and product solubility were related to **10**'s additional benzene ring or its lack of phenolic −OH, the synthesis of **11** was attempted; **11** is an analogue of **4** that simply removes the −OH and leaves the ethyl group intact. In this case, we were unable to purify **11** via trituration; recrystallization was attempted and was found to provide inconsistent results. From there, chromatography was considered, and typical solvents including hexanes, ethyl acetate, dichloromethane, and methanol were screened for their ability to pass **11** across normal-phase silica gel. The most polar conditions screened (20% methanol in dichloromethane) caused excessive streaking of **11**, but the desired product traveled uniformly when ammonium hydroxide was added to the mobile phase (final composition of 80% DCM, 18% MeOH, 2% NH_4OH). This provided insight that amino dihydropyrimidines that lack aryl substitution from the β-keto ester component undergo the aza-Biginelli with considerably lower efficiency (13% versus 55%) and provide additional purification challenges. With the synthesis of analogue **11** determined, the synthesis of **4** was reinitiated with the knowledge that flash chromatography would likely be necessary to produce pure product, and we were able to leverage this insight to produce **4** in 14% yield. While our yields of alkyl substituted products were far below the initial report of **4**,[7] we were pleased that they were closely aligned with other primary literature.[14−17]

Scheme 2. Synthesis of Amino Dihydropyrimidine Analogues

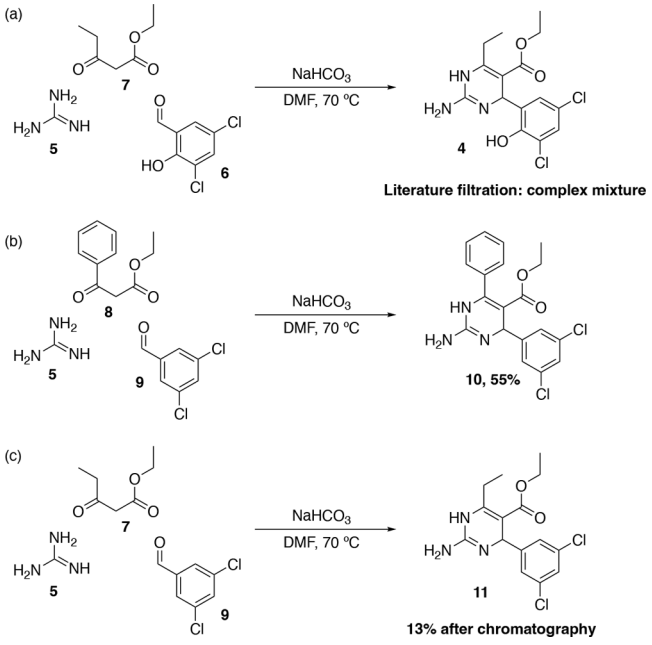

While our primary interest in the amino dihydropyrimidine chemotype was to evaluate its biological activity, low yields of the modified aza-Biginelli reaction were posing a barrier to this goal. To address this, reaction optimization was undertaken to investigate how modifications of temperature, solvent, time, reagent equivalents, bases, and energy input methods would impact the reaction's efficiency. We investigated this using quantitative analytical methods, where aliquots of the modified reaction mixtures were injected onto an HPLC and the product signal integration was compared to a standard curve (Figure S2). The most noteworthy changes came from lowering the temperature from 70 °C to 50 °C and increasing the equivalents of guanidine from 1.2 to 2.5 (full data are available in Table S1). A similar amount of product was produced when the reaction was run overnight at 50 or 70 °C,

https://doi.org/10.1021/acsomega.2c05071
ACS Omega 2022, 7, 37907−37916

but the HPLC chromatogram demonstrated a significant increase in the amount of decomposition products when the reaction was run at 70 °C. For that reason, other optimization changes were considered at 50 °C. The use of increased equivalents of guanidine has precedent to lower the production of Biginelli dimers,[18] and we were pleased to observe these relatively modest changes increased the yield of **4** to 30% (Scheme 3). This represents more than a doubling of the yield compared to our attempted reproduction of the literature precedent of **4** (14%),[7] a similar overall yield of alkyl-substituted amino dihydropyrimidines compared to the chemistry developed by the Wipf group,[20] and a higher yield than those in the primary literature published during the 1990s and early 2000s.[14−17] Further, as the aza-Biginelli reaction forms three bonds between the three separate reaction components, a 30% overall yield would imply a yield of 67% per bond formed. With these optimized conditions in hand (Scheme 3), focused libraries of amino dihydropyrimidines were proposed and prepared to examine their biological properties (synthesis and characterization details can be found in the Supporting Information).

Scheme 3. Optimized aza-Biginelli Reaction Conditions

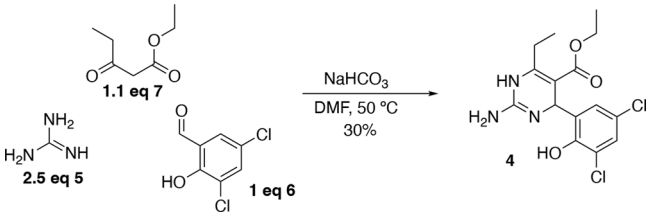

Characterization of Amino Dihydropyrimidine Products. During the application of the optimized reaction conditions to a range of dihydropyrimidine analogues, a complication arose regarding the characterization of some derivatives by NMR. The chromatographic purification of most analogues proceeded without issue, but some compounds appeared to have extensive amounts of impurities following chromatography. In these cases, recrystallization was attempted to purify the product-containing fractions but led to no purity improvements. After these challenges, it was postulated that the smaller set of signals may be due to the product existing as a mixture of guanidine tautomers (Figure 2a), as the splitting patterns and chemical shifts of the minor signals somewhat resembled the major NMR signals. While the amino dihydropyrimidine analogs are most commonly represented as tautomer **I**,[7,20−22] some reports note the mixture of **I** and **II**[14,15,18] and others describe tautomer **III** as the major isomer present when the compound is a guanidinium salt.[19] One

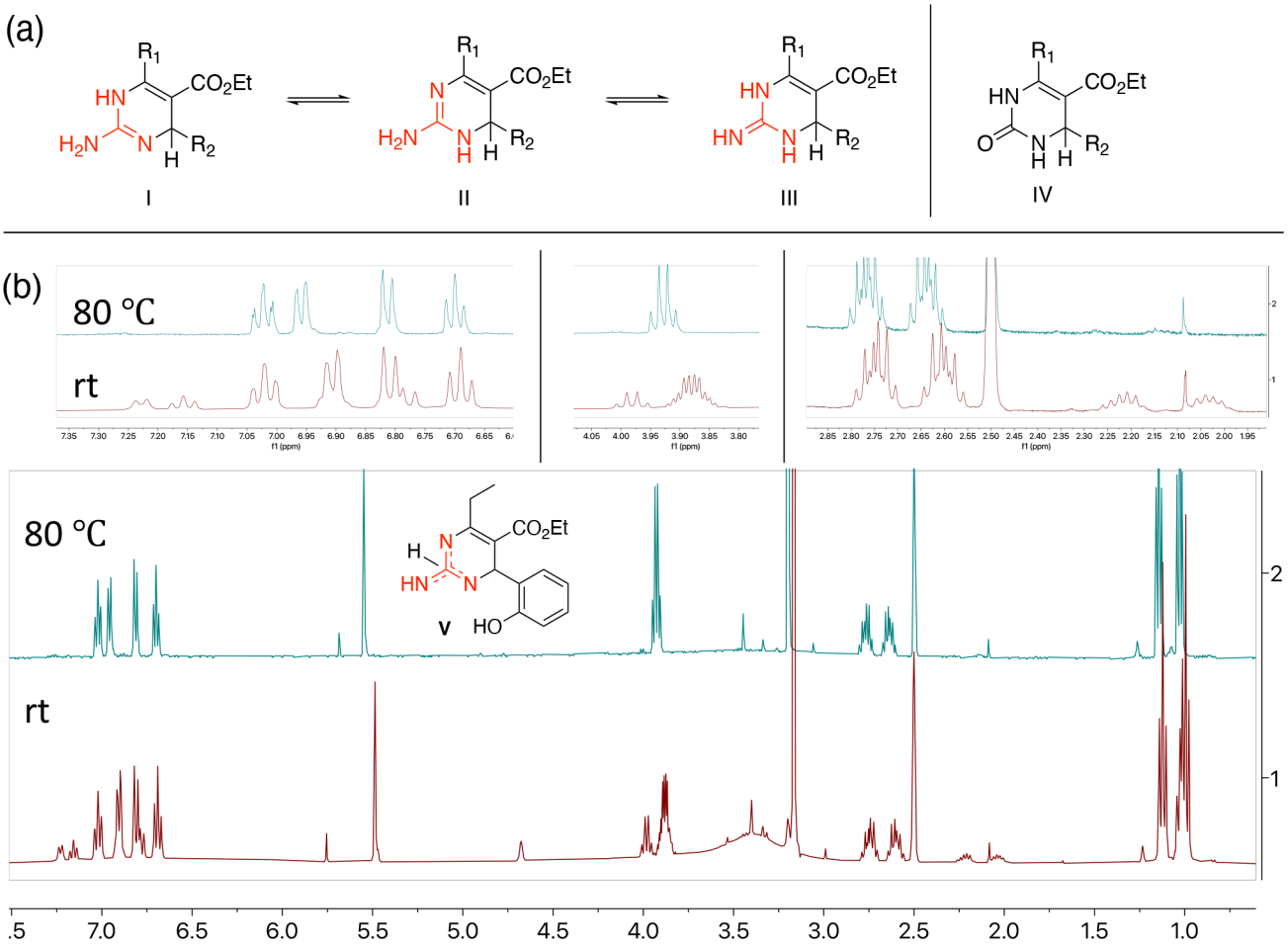

Figure 2. (a) Tautomeric states of amino dihydropyrimidine products (**I**−**III**) and the standard tautomer state of dihydropyrimidones (**IV**). (b) Variable-temperature ^{1}H NMR analysis of an amino dihydropyrimidine analog at room temperature (~23 °C) and 80 °C. Smaller sets of signals coalesce with larger signals when the temperature increases.

https://doi.org/10.1021/acsomega.2c05071
ACS Omega 2022, 7, 37907−37916

indicator of the tautomer identity is the splitting of the dihydropyridine's methine proton. In tautomer **I**, the proton is expected to be a singlet, while in tautomers **II** and **III** it can be split by the adjacent N−H; this is its most common splitting pattern in dihydropyrimidones **IV**, as they exist almost exclusively in that tautomer state. While this explanation seemed plausible, it is noteworthy that most amino dihydropyrimidine analogs showed no evidence of these tautomer mixtures (e.g., compound **4**). To investigate whether the unknown NMR signals were caused by the existence of tautomers in appreciable quantities, variable-temperature NMR spectroscopy was performed to increase the rate of exchange between the isomers, which we anticipated would cause an averaging of signals (Figure 2b shows the spectrum of the dihydropyrimidine product **V**, which exhibits tautomer signals). Indeed, the NMR spectrum of **V** at room temperature showed relatively significant tautomer signals associated with the dihydropyrimidine's arene signals (6.75−7.25 ppm), methine signal (4.68 ppm), methylene of the ethyl ester's signal (3.98 ppm), and methylene of the ethyl directly connected to the dihydropyrimidine's signals (diastereotopic minor signals, 2.27−2.16 and 2.07−1.98 ppm). When the temperature of the NMR was increased to 80 °C, the intensity of these signals diminished and they became almost indistinguishable (Figure 2b), further suggesting that the signals were due to a minor dihydropyrimidine tautomer. Additionally, the tautomer ratios differed when the NMR solvents were changed, being more significant in acetone-D_6 and less significant in DMSO-D_6 (the solvent used in Figure 2b). This temperature and solvent dependence of the concentrations of the tautomer in amidine- and guanidine-containing heterocycles has significant precedent,[23−27] but a limited amount is understood regarding this phenomenon with densely functionalized heterocycles such as aza-Biginelli reaction products. High-temperature NMR spectroscopy also proved useful in the ^{13}C NMR characterization, as the ^{13}C signals in some cases became more resolved at high temperatures and fewer scans were required to obtain a spectrum. These insights facilitated a smoother process during the synthesis, purification, and characterization of the compounds prior to the analysis of their biological activity.

Antibacterial Structure Activity Relationships. Dihydropyrimidine **4**'s initial report described the growth inhibition of methicillin sensitive *S. aureus* (2 μg/mL) and two strains of MRSA (9 μg/mL) and disclosed the synthesis of four modestly related analogues that were less biologically active (Figure 3a).[7] Examining these closely, the analogues with an arene in the R_2 position were limited to the dichlorophenol of **4** and a thiophene (Figure 3a, compound **iv**). As the other analogues of **4** were significantly less potent, we aimed to directly investigate the SAR of **4**. We began these efforts by constructing a focused library of compounds that systematically removed each of the dichlorophenol's substituents (**4b**−**4g**) or capped the phenol as a methoxy group (**4a**) to investigate the need for a hydrogen bond donor in that position (Figure 3b).

These compounds were screened in microdilution assays beside approved antibiotics carbenicillin, erythromycin, gentamycin, trimethoprim, and vancomycin, and minimum inhibitory concentrations (MICs) were determined for each compound (Table 1). Compound activity was measured in methicillin-sensitive *S. aureus* (ATCC 12600), hospital-acquired MRSA (ATCC 43300), and community-acquired MRSA (USA-300) to examine a range of *S. aureus* strains with

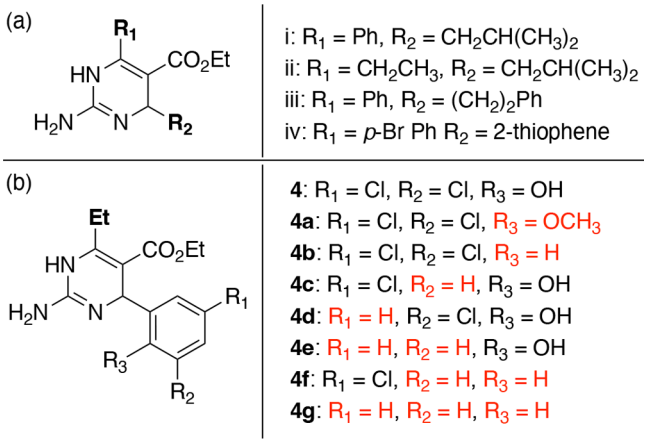

Figure 3. (a) Previously reported direct analogues of **4**. (b) Focused library evaluating the aryl substitution on compound **4** (differences are noted in red).

which we could compare **4**'s previously reported antibacterial activity. The inclusion of various strains is of clear importance, as the growth inhibition values for the FDA-approved antibiotics demonstrate that the strains have different properties that impact their susceptibility (Table 1). The data presented are the 50% growth inhibition MIC values (the concentration necessary to inhibit 50% of the bacterial growth), as these values aligned with **4**'s precedent.[7] We were pleased to note that **4** inhibited our strains of *S. aureus* with similar potency (8−16 μg/mL, Table 1) compared to its initial report (9 μg/mL in MRSA).[7] Additionally, modifications to the arene substituents had major impacts on the antibacterial activity. Notably, when the phenol was capped as a methyl ether (**4a**) or fully removed (**4b**), the growth inhibition potency increased to 4 μg/mL, a two- or fourfold increase in potency depending on the strain. Conversely, when the substituents were removed to leave a naked phenyl ring (**4g**), either no growth inhibition occurred (ATCC 12600) or a four- or eightfold higher concentration of the compound was required to inhibit bacterial growth (64 μg/mL in both MRSA strains). Our other modifications—leaving a single chlorine with the phenol intact (**4c** and **4d**), leaving only the phenol (**4e**), or leaving a single chlorine (**4f**)—also resulted in diminished potency compared to **4**. In all, this focused set of compounds shows that the substituents on this arene ring have a noteworthy ability to modulate the antibacterial activity of this compound class. While **4** was previously reported to lack mammalian toxicity,[7] we screened this focused library for hemolysis at 64 μg/mL and noted a total absence of hemolytic activity.

To examine the importance of the ethyl substituent on **4**, we prepared 16 additional compounds with arene modifications noted above while truncating the ethyl to a methyl or extending it to a phenyl ring (Figure 4).

These compounds were screened in microdilution assays against the same three strains of *S. aureus* (results in Table 2). Comparing the activity of **4** (8−16 μg/mL) to those of the methyl **12** and phenyl **13** analogues, the potency across the strains is generally similar or modestly lower (8−32 μg/mL). Further, none of the other analogues have potency gains to match the ethyl analogues (**4a** and **4b**, 4 μg/mL). Some of the trends matched; for example, the elimination of the phenol to form a dichloro arene provided the most potent inhibition

https://doi.org/10.1021/acsomega.2c05071
ACS Omega 2022, 7, 37907−37916

Table 1. Antibacterial Activity of Focused Library 1 (Figure 3) Measured as the Minimum Inhibitory Concentration (MIC)

									antibiotic controls[a]				
	4	4a	4b	4c	4d	4e	4f	4g	Carb	Emc	Gent	TMP	Vanc
methicillin-sensitive *S. aureus* (ATCC 12600)	8	4	4	16	32	64	16	>64[b]	0.5	0.5	2	16	1
methicillin-resistant *S. aureus* (ATCC 43300)	16	4	4	16	32	32	16	64	32	>64[b]	>64[b]	2	1
methicillin-resistant *S. aureus* (USA 300)	8	4	4	16	32	32	16	64	64	16	0.5	1	1

[a]Carb = carbenicillin; Emc = erythromycin; Gent = gentamycin; TMP = trimethoprim; and Vanc = vancomycin. [b]Testing concentrations higher than 64 μg/mL were not used due to compound solubility limitations.

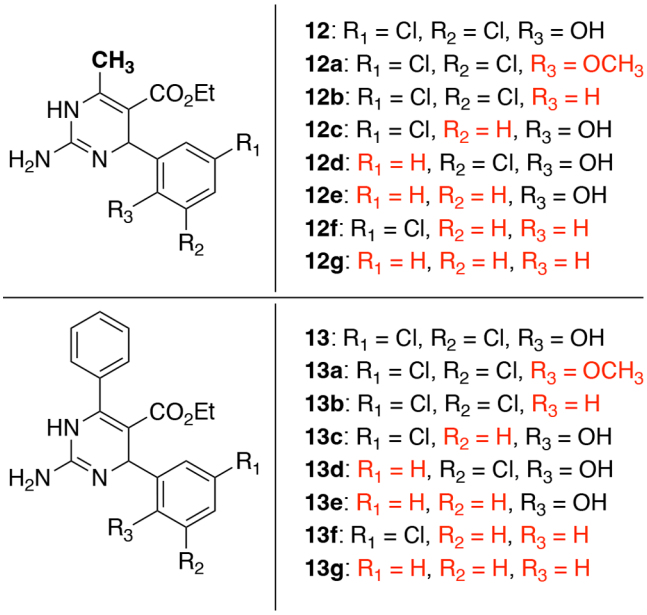

Figure 4. Focused library evaluating modifications to the ethyl and aryl substituents of compound 4.

across all three strains (8 μg/mL). Further, the elimination of all substituents on the diphenyl-substituted dihydropyrimidine **13g** matched the lack of activity noted in the ethyl analogue **4g**, where either >64 or 64 μg/mL was required to inhibit bacterial growth. Overall, the new compounds mostly indicated that the dihydropyrimidines had slightly enhanced activities with an ethyl group, but losses in potency when the ethyl group was changed to a phenyl ring or methyl group were modest. This indicates that this region of the molecule seems to have a smaller impact on the biological activity of these compounds. Additionally, these compounds were screened for hemolysis and showed no hemolytic activity at 64 μg/mL.

Dihydropyrimidones (**IV** in Figure 2a) have broad-ranging documented biological activity.[28] Therefore, we synthesized[29,30] urea- and thiourea-containing analogues of compounds **4**, **12**, and **13** to examine the impact of exchanging guanidine's exocyclic nitrogen with an oxygen or sulfur atom (compounds in Figure S3). These modifications would retain many of the steric and electronic properties of our bioactive dihydropyrimidines but eliminate their ability to donate hydrogen bonds from the exocyclic nitrogen. Thiourea analogues of **4** and **13** provided modest *S. aureus* growth inhibition at concentrations of 64 μg/mL, while the remaining analogues lacked any impact on growth at concentrations up to 64 μg/mL, the highest concentration tested due to solubility concerns. This indicates that the exocyclic nitrogen, and the guanidine moiety in general, is vitally important for the antibacterial activity of this compound class. Taken altogether, our focused compound libraries indicate which regions of the dihydropyrimidine lead compound **4** tolerate change and which parts are essential for bioactivity (Figure 5). Future

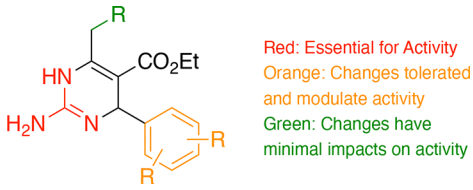

Figure 5. SAR trends revealed through the synthesis and biological evaluation of focused libraries.

compound libraries will take these SAR data into mind to (1) design compounds that maintain the guanidine, as it is essential for biological activity; (2) exhaustively employ a wide variety of benzaldehyde starting materials, going beyond the simple structural components present in lead compound **4**; and (3) make significant changes to **4**'s ethyl group to examine if other functional groups appreciably improve the activity.

Mechanism of Action Studies. Lead compound **4** and analogues thereof have molecular structures comparable to those of FDA approved medications that work by inhibiting DHFR (Figure 1), and some derivatives of **4** inhibit the growth of *S. aureus* with potencies similar to the DHFR-inhibiting antibiotic TMP (Table 1 and 2). A previous report[7] characterized **4** as an uncompetitive inhibitor of DHFR, and we intended to link the antibacterial activity observed in cell-based assays to target-based DHFR enzyme inhibition. Toward this goal, we expressed and purified recombinant *S.aureus* DHFR (*Sa*DHFR) from a pET 101D vector with a C-terminal histidine affinity tag (Figure S4).[31] Once purified, the enzyme was shown to exhibit standard Michaelis–Menten kinetics when the concentration of dihydrofolate was serially increased. Further, we showed the standard inhibition of DHFR activity

Table 2. Antibacterial Activity of Focused Library 2 (Figure 4) Measured as the Minimum Inhibitory Concentration (MIC)

	12	12a	12b	12c	12d	12e	12f	12g	13	13a	13b	13c	13d	13e	13f	13g
methicillin-sensitive *S. aureus* (ATCC 12600)	16	16	8	32	64	>64[a]	8	32	16	8	8	16	32	16	32	>64[a]
methicillin-resistant *S. aureus* (ATCC 43300)	32	16	8	32	32	>64[a]	8	32	16	8	8	16	32	16	16	>64
methicillin-resistant *S. aureus* (USA 300)	16	16	8	32	32	>64[a]	8	32	8	8	8	16	16	16	16	>64

[a]Testing concentrations higher than 64 μg/mL were not used due to compound solubility limitations.

https://doi.org/10.1021/acsomega.2c05071
ACS Omega 2022, 7, 37907−37916

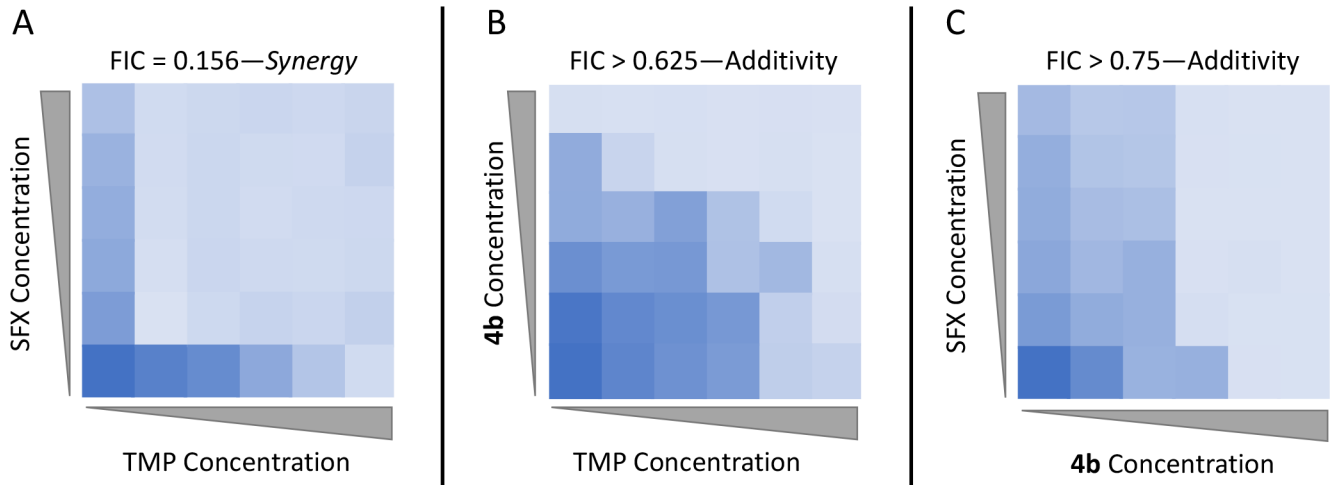

Figure 6. Checkerboard assay heat maps examining the synergistic, additive, or indifferent effects of (A) SFX and TMP, (B) **4b** with TMP, and (C) SFX with **4b**. Darker blue indicates more bacterial growth. FIC values less than 0.5 indicate synergy, while FIC values greater than 0.5 indicate additive effects.

via the addition of TMP, a well-characterized competitive inhibitor of DHFR activity (Figure S5). At this point the enzyme was considered standardized, and we began screening our compound libraries to examine the ability of our compounds to inhibit the enzyme. We were surprised to note that none of our dihydropyrimidine analogs showed significant DHFR inhibition at concentrations as high as 64 μg/mL, indicating that they may derive their antibacterial properties from a secondary mechanism. As our *Sa*DHFR expression construct was different from those in previous reports, we desired secondary measures to potentially demonstrate that our compounds perturb the folate pathway. Further, as our compound has similar features to dihydrofolate and its known inhibitors, we considered that it could be inhibiting some other step of the folate synthesis pathway. To scrutinize this idea, we examined whether our most potent compound **4b** could have synergy with TMP or sulfamethoxazole (SFX), an inhibitor of dihydropteroate synthetase that is known to provide synergistic antibacterial effects with DHFR inhibitors such as TMP.[32] Checkerboard assays were performed to calculate fractional inhibitory concentrations (FICs), where an FIC of less than 0.5 indicates synergy, FIC values between 0.5 and 4 indicate additivity or indifference, and an FIC greater than 4 indicates an antagonistic impact.[33] The initial examination of SFX with TMP validated the assay and showed clear synergy between the components, with a FIC of 0.156 (Figure 6A). To investigate whether **4b** was impacting the folate pathway at DHFR or elsewhere, checkerboard assays were performed by combining **4b** with both TMP (Figure 6B) and SFX (Figure 6C). In both cases, FIC values between 0.5 and 1 indicated the antibacterial agents likely had additive activity, but this failed to show any link between our functionalized dihydropyrimidines and the folate pathway.

To examine compound−DHFR interactions as directly as possible, *in vitro* assays were planned that would explore a direct interaction between our ligands and *Sa*DHFR. Differential scanning fluorimetry (DSF) and crystallography were pursued. The DSF assay was first performed with trimethoprim, revealing a dose-dependent increase in the temperature of thermal denaturation (T_m). This effect was further enhanced by the addition of the saturating cofactor NADPH. The presence of compounds at both available large binding pockets completely stabilizes the enzyme, resulting in a transition in the T_m of 10 μM *Sa*DHFR from 45.3 °C to 53.3 °C at saturating (≥800 μM) TMP, 56.3 °C at saturating (≥100 μM) NADPH, and 75.6 °C when both are saturating (Figure S6). The addition of compound **4** at concentrations up to 800 μM in combination with any other compound, including in combinations of both NADPH and folate pocket-binding compounds (TMP or 400 μM 2,4-diaminopyrimidine), did not impact the T_m value.

Attempts to cocrystallize or soak **4** also failed to return any structures containing density indicative of **4** binding. The *Sa*DHFR structure was previously determined with NADPH, TMP, and other folate-mimicking derivatives.[34−42] The inclusion of **4** at saturating concentrations with *Sa*DHFR did not yield crystals under previously determined conditions, and broad screens for new conditions did not successfully produce visible protein crystals. Using the previous conditions (10 mg/mL SaDHFR), we grew crystals with NADPH (1.1 mM) and TMP (saturating) in addition to **4** at saturating conditions. While crystals were readily obtained, the analysis of the resulting electron density failed to produce any indications of additional bound molecules. These crystals were then soaked in an excess of **4** (at saturating concentrations) for up to one month and showed no evidence of damage. The resulting diffraction was extended to a comparable resolution, and no additional density was noted that could correspond to the added compound.

Despite the useful antibacterial activity and SARs elucidated in this study, the mechanism by which the functionalized dihydropyrimidine analogs act appears to be unclear. Despite dihydropyrimidine's structural resemblance to dihydrofolate, trimethoprim, and other compounds that interact with DHFR, our assays show a lack of connection. In sum, whole-cell checkerboard assays showed no synergy with other inhibitors that interacted with the folate pathway, and *in vitro* assays examining compound−DHFR interactions directly using enzyme kinetics, DSF, and crystallography lacked any evidence of interactions with the enzyme. As the compounds do produce significant antibacterial activity, one emphasis of future efforts will be to evaluate alternative mechanisms by which the compounds may exert their effect, including the synthesis and use of dihydropyrimidine-based photoaffinity

https://doi.org/10.1021/acsomega.2c05071
ACS Omega 2022, 7, 37907−37916

probes that may illuminate a molecular target. Additionally, other biophysical methods, including saturation transfer difference NMR, may be used to examine interactions between our compounds and their molecular target. Further, antibacterial SAR studies currently underway are aimed at improving the antibacterial potency while simultaneously exploring sites for the addition of photocleavable reactive moieties, and these data will be reported in due course.

SUMMARY

We have explored the potential biological importance of a class of functionalized dihydropyrimidine molecules. Toward this effort, the optimization of the aza-Biginelli reaction and purification conditions facilitated reproducibility in analogue synthesis, and the use of variable-temperature NMR spectroscopy simplified characterization efforts. The preparation of focused chemical libraries of the lead compounds and their use in 96-well plate microdilution assays provided insight into the SAR of antibacterial activity, indicating which components of the lead compound were likely to prove most fertile toward future analogue synthesis efforts. Despite the promise of lead compound **4** as an antibacterial compound that works via DHFR inhibition, our efforts indicate that although functionalized dihydropyrimidine analogues derived from the lead have useful antibacterial activity, the mechanism by which they act remains unclear. Future studies will focus on improving the antibacterial activity of this chemotype while examining the mechanism of its biological activity.

ASSOCIATED CONTENT

Supporting Information

The Supporting Information is available free of charge at https://pubs.acs.org/doi/10.1021/acsomega.2c05071.

Chemical synthesis, MIC assays, enzyme kinetics, differential scanning fluorimetry, crystallography, and NMR spectra of compounds (PDF)

AUTHOR INFORMATION

Corresponding Author

Matthew C. O'Reilly − *Department of Chemistry, Villanova University, Villanova, Pennsylvania 19085, United States;* orcid.org/0000-0002-9175-4179; Email: matthew.oreilly@villanova.edu

Authors

Zachary W. Boyer − *Department of Chemistry, Villanova University, Villanova, Pennsylvania 19085, United States*

Hannah Kessler − *Department of Chemistry, Villanova University, Villanova, Pennsylvania 19085, United States*

Hannah Brosman − *Department of Chemistry, Villanova University, Villanova, Pennsylvania 19085, United States*

Kirsten J. Ruud − *Department of Chemistry and Biotechnology, University of Wisconsin−River Falls, River Falls, Wisconsin 54022, United States;* Present Address: Department of Chemistry, University of California−Irvine, Irvine, California 92697, United States

Alan F. Falkowski − *Department of Chemistry and Biotechnology, University of Wisconsin−River Falls, River Falls, Wisconsin 54022, United States;* Present Address: Bethel University, Arden Hills, Minnesota 55125, United States

Constance Viollet − *Department of Chemistry, Villanova University, Villanova, Pennsylvania 19085, United States*

Christina R. Bourne − *Department of Chemistry and Biochemistry, University of Oklahoma, Norman, Oklahoma 73019, United States;* orcid.org/0000-0001-6192-3392

Complete contact information is available at: https://pubs.acs.org/10.1021/acsomega.2c05071

Author Contributions

#Z.W.B. and H.K. contributed equally.

Notes

The authors declare no competing financial interest.

ACKNOWLEDGMENTS

M.C.O. acknowledges an NIH AREA grant (1R15GM140412-01) for research support and Villanova University for generous start-up funding. The NMR and MS instrumentation at Villanova is supported by Major Research Instrumentation grants from the National Science Foundation (CHE-1827930 and CHE-2018399). The following reagents were provided by the Network on Antimicrobial Resistance in *Staphylococcus aureus* (NARSA) for distribution by BEI Resources, NIAID, NIH: *Staphylococcus aureus*, strain USA300-0114, NR-46070. The Biomolecular Structure Core is supported in part by an Institutional Development Award (IDeA) from the National Institute of General Medical Sciences of the National Institutes of Health (Award P20GM103640), the National Science Foundation (Award 0922269), and the University of Oklahoma Department of Chemistry and Biochemistry.

REFERENCES

(1) Boucher, H. W.; Talbot, G. H.; Bradley, J. S.; Edwards, J. E.; Gilbert, D.; Rice, L. B.; Scheld, M.; Spellberg, B.; Bartlett, J. Bad Bugs, No Drugs: No ESKAPE! An Update from the Infectious Diseases Society of America. *Clin. Infect. Dis.* **2009**, *48* (1), 1−12.

(2) Centers for Disease Control and Prevention. *Antibiotic Resistance Threats in the United States, 2013*; U.S. Department of Health and Human Services: Atlanta, GA, 2013.

(3) Centers for Disease Control and Prevention. *Antibiotic Resistance Threats in the United State, 2019*; U.S. Department of Health and Human Services: Atlanta, GA, 2019.

(4) Nelson, D. L.; Cox, M. M. *Lehninger Principles of Biochemistry*, 4th ed.; W. H. Freeman and Company: New York, NY, 2005.

(5) Bush, K.; Bradford, P. A. *β*-Lactams and *β*-Lactamase Inhibitors: An Overview. *Cold Spring Harb. Perspect. Med.* **2016**, *6*, a025247.

(6) Ibrahim, M. E.; Abbas, M.; Al-Shahrai, A. M.; Elamin, B. K. Phenotypic Characterization and Antibiotic Resistance Patterns of Extended-Spectrum *β* -Lactamase- and AmpC *β* -Lactamase-Producing Gram-Negative Bacteria in a Referral Hospital, Saudi Arabia. *Can. J. Infect. Dis. Med. Microbiol.* **2019**, *2019*, 1−9.

(7) Wyatt, E. E.; Galloway, W. R. J. D.; Thomas, G. L.; Welch, M.; Loiseleur, O.; Plowright, A. T.; Spring, D. R. Identification of an Anti-MRSA Dihydrofolate Reductase Inhibitor from a Diversity-Oriented Synthesis. *Chem. Commun. (Camb).* **2008**, 4962−4964.

(8) He, J.; Qiao, W.; An, Q.; Yang, T.; Luo, Y. Dihydrofolate Reductase Inhibitors for Use as Antimicrobial Agents. *Eur. J. Med. Chem.* **2020**, *195*, 112268.

(9) Wróbel, A.; Arciszewska, K.; Maliszewski, D.; Drozdowska, D. Trimethoprim and Other Nonclassical Antifolates an Excellent Template for Searching Modifications of Dihydrofolate Reductase Enzyme Inhibitors. *J. Antibiot. (Tokyo).* **2020**, *73* (1), 5−27.

(10) Burchall, J. J.; Hitchings, G. H. Inhibitor Binding Analysis of Dihydrofolate Reductases from Various Species. *Mol. Pharmacol.* **1965**, *1* (2), 126−136.

(11) Roth, B.; Aig, E.; Rauckman, B. S.; Strelitz, J. Z.; Phillips, A. P.; Ferone, R.; Bushby, S. R. M.; Sigel, C. W. 2,4-Diamino-5-Benzylpyrimidines and Analogues as Antibacterial Agents. 5. 3′,5′-Dimethoxy-4′-Substituted-Benzyl Analogues of Trimethoprim. *J. Med. Chem.* **1981**, *24* (8), 933−941.
(12) Dietrich, S. W.; Blaney, J. M.; Reynolds, M. A.; Jow, P. Y. C.; Hansch, C. Quantitative Structure-Selectivity Relationships. Comparison of the Inhibition of Escherichia Coli and Bovine Liver Dihydrofolate Reductase by 5-(Substituted-Benzyl)-2,4-Diaminopyrimidines. *J. Med. Chem.* **1980**, *23* (11), 1205−1212.
(13) Wyatt, E. E.; Fergus, S.; Galloway, W. R. J. D.; Bender, A.; Fox, D. J.; Plowright, A. T.; Jessiman, A. S.; Welch, M.; Spring, D. R. Skeletal Diversity Construction via a Branching Synthetic Strategy. *Chem. Commun. (Camb).* **2006**, *31*, 3296−3298.
(14) Cho, H.; Shima, K.; Hayashimatsu, M.; Ohnaka, Y.; Mizuno, A.; Takeuchi, Y. Synthesis of Novel Dihydropyrimidines and Tetrahydropyrimidines. *J. Org. Chem.* **1985**, *50* (22), 4227−4230.
(15) Atwal, K. S.; Rovnyak, G. C.; Schwartz, J.; Moreland, S.; Hedberg, A.; Gougoutas, J. Z.; Malley, M. F.; Floyd, D. M. Dihydropyrimidine Calcium Channel Blockers: 2-Heterosubstituted 4-Aryl-l,4-Dihydro-6-Methyl-5-Pyrimidinecarboxylic Acid Esters as Potent Mimics of Dihydropyridines. *J. Med. Chem.* **1990**, *33* (5), 1510−1515.
(16) Atwal, K. S.; Rovnyak, G. C.; O'Reilly, B. C.; Schwartz, J. Substituted 1,4-Dihydropyrimidines. 3. Synthesis of Selectively Functionalized 2-Hetero-1,4-Dihydropyrimidines. *J. Org. Chem.* **1989**, *54* (25), 5898−5907.
(17) Kappe, C. O. Highly Versatile Solid Phase Synthesis of Biofunctional 4-Aryl-3,4- Dihydropyrimidines Using Resin-Bound Isothiourea Building Blocks and Multidirectional Resin Cleavage. *Bioorg. Med. Chem. Lett.* **2000**, *10*, 49−51.
(18) Milcent, R.; Malanda, J.-C.; Barbier, G.; Vaissermann, J. Synthesis of Ethyl 2-aminodihydro-5-pyrimidinecar-boxylate Derivatives and 3,7-Diethyoxycarbonyl-4,6-Dihydro-2,4,6,8-Tetraaryl-1*H*-Pyrimido[1,2-*a*]Pyrimidines. *J. Heterocycl. Chem.* **1997**, *34*, 329−336.
(19) Nilsson, B. L.; Overman, L. E. Concise Synthesis of Guanidine-Containing Heterocycles Using the Biginelli Reaction. *J. Org. Chem.* **2006**, *71* (20), 7706−7714.
(20) Arnold, D. M.; Laporte, M. G.; Anderson, S. M.; Wipf, P. Condensation Reactions of Guanidines with Bis-Electrophiles: Formation of Highly Nitrogenous Heterocycles. *Tetrahedron* **2013**, *69* (36), 7719−7731.
(21) Ahmad, M. J.; Hassan, S. F.; Nisa, R. U.; Ayub, K.; Nadeem, M. S.; Nazir, S.; Ansari, F. L.; Qureshi, N. A.; Rashid, U. Synthesis, in Vitro Potential and Computational Studies on 2-Amino-1, 4-Dihydropyrimidines as Multitarget Antibacterial Ligands. *Med. Chem. Res.* **2016**, *25* (9), 1877−1894.
(22) Felluga, F.; Benedetti, F.; Berti, F.; Drioli, S.; Regini, G. Efficient Biginelli Synthesis of 2-Aminodihydropyrimidines under Microwave Irradiation. *Synlett* **2018**, *29* (8), 1047−1054.
(23) Ghiviriga, I.; El-Gendy, B. E. D. M.; Steel, P. J.; Katritzky, A. R. Tautomerism of Guanidines Studied by 15N NMR: 2-Hydrazono-3-Phenylquinazolin-4(3H)-Ones and Related Compounds. *Org. Biomol. Chem.* **2009**, *7* (19), 4110−4119.
(24) Caine, B. A.; Dardonville, C.; Popelier, P. L. A. Prediction of Aqueous p K a Values for Guanidine-Containing Compounds Using Ab Initio Gas-Phase Equilibrium Bond Lengths. *ACS Omega* **2018**, *3* (4), 3835−3850.
(25) Cho, H.; Iwashita, T.; Ueda, M.; Mizuno, A.; Mizukawa, K.; Hamaguchi, M. On the Tautomerism of Dihydropyrimidines: The Influence of the 2- and 5-Substituents on the Observation of Tautomers. *J. Am. Chem. Soc.* **1988**, *110* (14), 4832−4834.
(26) Steel, P. J. Heterocyclic Tautomerism. V [1]. 2-Guanidinobenzimidazole. *J. Heterocycl. Chem.* **1991**, *28*, 1817−1818.
(27) Jackman, L. M.; Jen, T. 1H and 13C Nuclear Magnetic Resonance Studies on the Tautomerism, Geometrical Isomerism, and Conformation of Some Cyclic Amidines, Guanidines, and Related Systems. *J. Am. Chem. Soc.* **1975**, *97*, 2811−2818.
(28) Kaur, R.; Chaudhary, S.; Kumar, K.; Gupta, M. K.; Rawal, R. K. Recent Synthetic and Medicinal Perspectives of Dihydropyrimidones: A Review. *Eur. J. Med. Chem.* **2017**, *132*, 108−134.
(29) Hu, E. H.; Sidler, D. R.; Dolling, U. H. Unprecedented Catalytic Three Component One-Pot Condensation Reaction: An Efficient Synthesis of 5-Alkoxycarbonyl-4-Aryl-3,4-Dihydropyrimidin-2(1H)-Ones. *J. Org. Chem.* **1998**, *63* (10), 3454−3457.
(30) Mahgoub, S.; Kotb El-Sayed, M. I.; El-Shehry, M. F.; Mohamed Awad, S.; Mansour, Y. E.; Fatahala, S. S. Synthesis of Novel Calcium Channel Blockers with ACE2 Inhibition and Dual Antihypertensive/Anti-Inflammatory Effects: A Possible Therapeutic Tool for COVID-19. *Bioorg. Chem.* **2021**, *116* (May), 105272.
(31) Bourne, C. R.; Barrow, E. W.; Bunce, R. A.; Bourne, P. C.; Berlin, K. D.; Barrow, W. W. Inhibition of Antibiotic-Resistant Staphylococcus Aureus by the Broad-Spectrum Dihydrofolate Reductase Inhibitor RAB1. *Antimicrob. Agents Chemother.* **2010**, *54* (9), 3825−3833.
(32) Bushby, S. R. M. Trimethoprim-Sulfamethoxazole: In Vitro Microbiological Aspects. *J. Infect. Dis.* **1973**, *128*, S442−S462.
(33) Pillai, S. K.; Moellering, R. C., Jr.; Eliopoulos, G. M. Antimicrobial Combinations. In *Antibiotics in Laboratory Medicine*, 5th ed.; Lorain, V.,, Ed.; Lippincott Williams & Wilkins Co.: Philadelphia, PA, 2005; pp 365−440.
(34) Oefner, C.; Parisi, S.; Schulz, H.; Lociuro, S.; Dale, G. E. Inhibitory Properties and X-Ray Crystallographic Study of the Binding of AR-101, AR-102 and Iclaprim in Ternary Complexes with NADPH and Dihydrofolate Reductase from Staphylococcus Aureus. *Acta Crystallogr. D* **2009**, *65* (8), 751−757.
(35) Oefner, C.; Bandera, M.; Haldimann, A.; Laue, H.; Schulz, H.; Mukhija, S.; Parisi, S.; Weiss, L.; Lociuro, S.; Dale, G. E. Increased Hydrophobic Interactions of Iclaprim with Staphylococcus Aureus Dihydrofolate Reductase Are Responsible for the Increase in Affinity and Antibacterial Activity. *J. Antimicrob. Chemother.* **2009**, *63* (4), 687−698.
(36) Reeve, S. M.; Gainza, P.; Frey, K. M.; Georgiev, I.; Donald, B. R.; Anderson, A. C. Protein Design Algorithms Predict Viable Resistance to an Experimental Antifolate. *Proc. Natl. Acad. Sci. U.S.A.* **2015**, *112* (3), 749−754.
(37) Reeve, S. M.; Si, D.; Krucinska, J.; Yan, Y.; Viswanathan, K.; Wang, S.; Holt, G. T.; Frenkel, M. S.; Ojewole, A. A.; Estrada, A.; Agabiti, S. S.; Alverson, J. B.; Gibson, N. D.; Priestley, N. D.; Wiemer, A. J.; Donald, B. R.; Wright, D. L. Toward Broad Spectrum Dihydrofolate Reductase Inhibitors Targeting Trimethoprim Resistant Enzymes Identified in Clinical Isolates of Methicillin Resistant Staphylococcus Aureus. *ACS Infect. Dis.* **2019**, *5* (11), 1896−1906.
(38) Lombardo, M.N.; G-Dayanandan, N.; Keshipeddy, S.; Zhou, W.; Si, D.; Reeve, S.M.; Alverson, J.; Barney, P.; Walker, L.; Hoody, J.; Priestley, N.D.; Obach, R.S.; Wright, D.L. Structure-Guided in Vitro to in Vivo Pharmacokinetic Optimization of Propargyl-Linked Antifolates. *Drug Metab. Dispos.* **2019**, *47* (9), 995−1003.
(39) Li, X.; Hilgers, M.; Cunningham, M.; Chen, Z.; Trzoss, M.; Zhang, J.; Kohnen, L.; Lam, T.; Creighton, C.; Gc, K.; Nelson, K.; Kwan, B.; Stidham, M.; Brown-Driver, V.; Shaw, K. J.; Finn, J. Structure-Based Design of New DHFR-Based Antibacterial Agents: 7-Aryl-2,4-Diaminoquinazolines. *Bioorg. Med. Chem. Lett.* **2011**, *21* (18), 5171−5176.
(40) Bourne, C. R.; Barrow, E. W.; Bunce, R. A.; Bourne, P. C.; Berlin, K. D.; Barrow, W. W. Inhibition of Antibiotic-Resistant Staphylococcus Aureus by the Broad-Spectrum Dihydrofolate Reductase Inhibitor RAB1. *Antimicrob. Agents Chemother.* **2010**, *54* (9), 3825−3833.
(41) Reeve, S. M.; Scocchera, E. W.; G-Dayanadan, N.; Keshipeddy, S.; Krucinska, J.; Hajian, B.; Ferreira, J.; Nailor, M.; Aeschlimann, J.; Wright, D. L.; Anderson, A. C. MRSA Isolates from United States Hospitals Carry DfrG and DfrK Resistance Genes and Succumb to Propargyl-Linked Antifolates. *Cell Chem. Biol.* **2016**, *23* (12), 1458−1467.
(42) Heaslet, H.; Harris, M.; Fahnoe, K.; Sarver, R.; Putz, H.; Chang, J.; Subramanyam, C.; Barreiro, G.; Miller, J. R. Structural Comparison

https://doi.org/10.1021/acsomega.2c05071
ACS Omega 2022, 7, 37907−37916

of Chromosomal and Exogenous Dihydrofolate Reductase from Staphylococcus Aureus in Complex with the Potent Inhibitor Trimethoprim. *Proteins Struct. Funct. Bioinforma.* **2009**, *76* (3), 706−717.

https://doi.org/10.1021/acsomega.2c05071
ACS Omega 2022, 7, 37907−37916